Bulk moduli and equations of state of ice VII and ice VIII

S. Klotz, K. Komatsu, H. Kagi, K. Kunc, A. Sano-Furukawa, S. Machida, T. Hattori

Bulk moduli and equations of state of ice VII and ice VIII

S. Klotz,[1,*] K. Komatsu,[2] H. Kagi,[2] K. Kunc,[1] A. Sano-Furukawa,[3] S. Machida,[4] and T. Hattori[3]

[1]*IMPMC, UMR 7590, Université P&M Curie, 4 Place Jussieu, F-75252 Paris, France*

[2]*Geochemical Research Center, Graduate School of Science, The University of Tokyo, 7-3-1 Hongo, Bunkyo-ku, Tokyo 113-0033, Japan*

[3]*J-PARC Center, Japan Atomic Energy Agency, 2-4 Shirakata, Tokai, Naka, Ibaraki 319-1195, Japan*

[4]*CROSS-Tokai, Research Centre for Neutron Science and Technology, 162-1 Shirakata, Tokai, Naka, Ibaraki 319-1106, Japan*

(Received 5 January 2017; revised manuscript received 7 April 2017; published 30 May 2017)

The compression behavior of deuterated ice VII and VIII was investigated by high pressure neutron scattering in the pressure range 2–13.7 GPa between 93 and 300 K. We establish equations of state which contain accurate values for the bulk moduli B_0, their pressure derivatives B_0^t, as well as the ambient pressure volume V_0. These equations of state hold over a large part of the stability domain of ice VII, by comparison with available x-ray data, and to at least ≈13 GPa for ice VIII. They are indistinguishable at low pressures, but beyond ≈7 GPa and at low temperatures ice VIII appears to become stiffer than expected. This might be related to an anomalous phonon hardening observed previously in ice VIII in this P/T range [D. D. Klug *et al.*, Phys. Rev. B **70**, 144113 (2004)].

Ice VII and VIII are the dominant high pressure phases of solid water. At 300 K, ice VII is stable between 2 and ≈70 GPa where it transforms continuously into hydrogen-centered ice X. Upon cooling to below ≈270 K it converts to its hydrogen-ordered form ice VIII which is stable down to 0 K. The compressional behavior of these two phases has been studied by several groups [1–15] up to the megabar range. These were mainly carried out by x-ray diffraction techniques in a diamond anvil cell (DAC) providing density as a function of pressure, and focused almost exclusively on ice VII which does not require cryogenic techniques. Fits to the $V(P)$ data using various types of equation of state (EoS) relations are expected to give the bulk modulus B_0, its pressure derivative B_0^t, and the ambient-pressure volume (density) V_0. But, although these equations of state all give acceptable fits to the data over the considered pressure range, the extracted parameters scatter strongly between different measurements. The reported bulk moduli of ice VII, for example, scatter between 4–5 GPa [11–13] and 24 GPa [3], and even in the most recent work vary between 13 GPa [14] and 21 GPa [15]. It hence appears that most of the reported equations of state are merely fits to $V(P)$ data with little physical significance concerning B_0, B_0^t, and V_0. It should be noted that ice VII can be decompressed to ambient pressure (recovered) [16] and that therefore B_0, B_0^t, and V_0 are well-defined thermodynamic material properties. Equations of state with unphysical parameters are not very useful for drawing any conclusions on binding properties at a microscopic level. They can hardly be compared with theory, and they cannot be extended significantly beyond the pressure range they were established for.

Here we present equations of state of ice VII at 298 K and ice VIII at low temperatures to 93 K which give physically meaningful values for B_0, B_0^t, and V_0 which are consistent with measured values on recovered samples. Our EoS is based on high pressure neutron diffraction data between 2 and 13.7 GPa, using lead as pressure marker, similar to previous experiments [14] but with a significantly extended pressure range. Compared to DAC measurements, this approach has various advantages. The spheroidal pressure chamber used in such a setup is known to produce an almost homogeneous pressure distribution [17], contrary to the situation in DAC work where pressure differences of typically 10% are observed [7]. Also, the bulk modulus of Pb is similar to that of the sample which eliminates the possibility of false pressure reading through the "Lamé effect" [18]. The pressure determined by Pb was recently calibrated to the NaCl scale and gives an accuracy on pressure which is comparable to that of the ruby scale, if not better [19].

Neutron diffraction measurements were carried out on two sample loadings at the high pressure beamline PLANET [20] at MLF, the Japan Proton Accelerator Research Complex (J-PARC), Tokai, Ibaraki, Japan. Both runs used double-toroidal sintered diamond anvils [21], encapsulating TiZr gaskets, deuterated water (99.6% D) from Eurisotop (France), and highly pure lead from New Metals and Chemicals Ltd. The first loading was entirely dedicated to ice VII at 298 K and used a VX4-type Paris-Edinburgh load frame [22] with the position of the sample (which is critical for accurate determination of lattice parameters) maintained to within ±0.1 mm relative to the laboratory frame using a previously determined calibration of the position as a function of load. The second loading applied a variable-temperature "Mito" system [23] and sintered diamond anvils with reduced sample volume compared to the first loading. In these measurements the sample position was determined by a scan along the beam direction and monitoring the scattered intensity of the sample, again to within ±0.1 mm. In both loadings about 1 mm^3 lead was cut into several pieces and distributed across the sample chamber. Lattice parameters (hence unit cell volumes) of ice VII/VIII and Pb were determined from Rietveld refinements as shown in Figs. 1 and 2. Due to the small sample volume in the second loading the diffraction patterns in these measurements contain reflections from the anvil material, i.e., diamond. This was considered as an additional phase and included in the fits. The refinements were carried out using Fullprof [24] based on the known structures of ice VII (space group $Pn\bar{3}m$) with O at (0.25,0.25,0.25) and D at (0.41,0.41,0.41) with 50% occupancy, ice VIII (space group $I4_1/amd$) with O at (0,1/4,0.10) and D at (0,0.43,0.21), Pb (space group $Fm\bar{3}m$),

*Corresponding author: stefan.klotz@impmc.upmc.fr

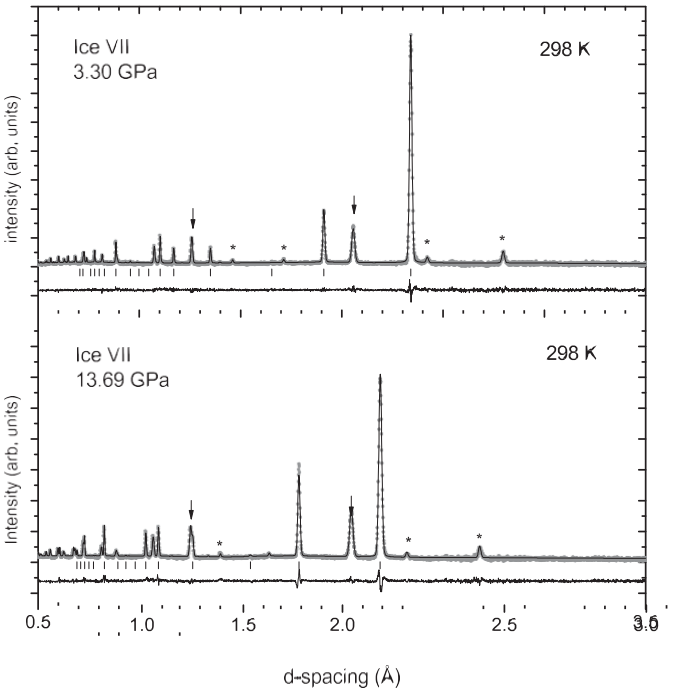

FIG. 1. Neutron diffraction patterns of ice VII collected at 298 K, at the lowest and highest pressures of loading 2. The lines through the data (dots) are results of Rietveld fits. Tick marks are at positions of Bragg reflections of the sample. Asterisks indicate strongest reflections of the lead pressure marker and the arrows point to the strongest reflections of diamond, the anvil material. Accumulation times are 30 min.

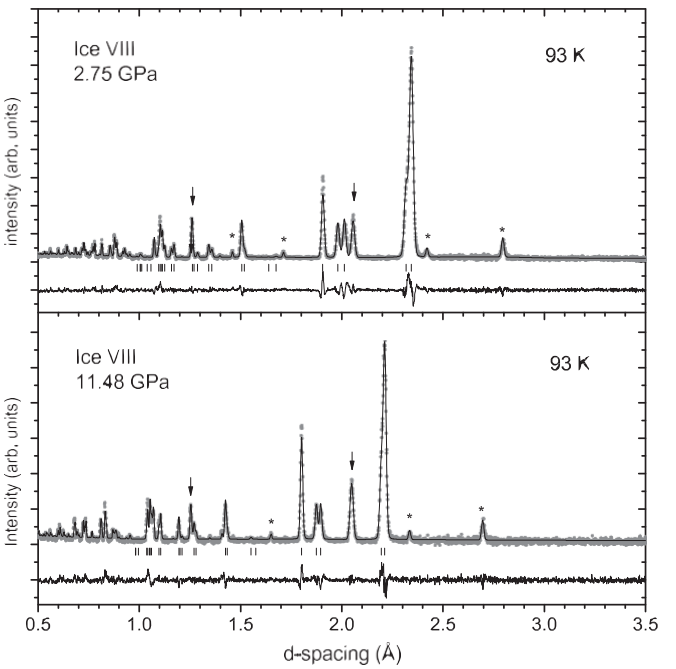

FIG. 2. Neutron diffraction patterns of ice VIII collected at 93 K, at the lowest and highest pressures. The lines through the data (dots) are results of Rietveld fits. Tick marks are at positions of Bragg reflections of the sample. Asterisks indicate strongest reflections of the lead pressure marker and the arrows point to the strongest reflections of diamond, the anvil material. Accumulation times are 30 min.

TABLE I. Measured lattice parameters of ice VII and Pb at 298 K and corresponding pressures.

Run	a_{VII} (Å)	V_{VII} (Å^3)	a_{Pb} (Å)	P (GPa)
24331	3.3581(1)	37.868(3)	4.878(1)	2.10(3)
24332	3.3578(1)	37.860(3)	4.879(1)	2.09(3)
24333	3.3373(1)	37.169(2)	4.865(1)	2.57(3)
24334	3.3160(1)	36.463(2)	4.846(1)	3.21(3)
24335	3.2900(1)	35.611(2)	4.828(1)	3.88(4)
24336	3.2634(1)	34.753(2)	4.806(1)	4.78(4)
24337	3.2405(1)	34.014(2)	4.785(1)	5.66(4)
24338	3.2233(1)	33.489(2)	4.770(1)	6.38(4)
24339	3.2044(1)	32.904(2)	4.752(1)	7.23(5)
24340	3.1805(1)	32.174(2)	4.730(1)	8.36(5)
24342	3.1315(2)	30.707(4)	4.682(3)	11.09(16)
24343	3.1318(2)	30.717(4)	4.681(3)	11.16(21)
30598	3.3096(1)	36.252(2)	4.844(1)	3.30(2)
30608	3.3081(1)	36.203(2)	4.843(1)	3.34(3)
30615	3.2503(1)	34.337(4)	4.794(2)	5.33(8)
30627	3.2042(1)	32.896(4)	4.751(2)	7.27(9)
30639	3.1456(2)	31.126(5)	4.696(2)	10.28(14)
30648	3.1276(1)	30.593(3)	4.677(1)	11.44(8)
30660	3.0962(1)	29.683(2)	4.643(1)	13.69(5)

and diamond (space group $Fd3m$), as well as a minimum of refineable parameters. Apart from lattice parameters, these are the fractional atomic coordinate of O (phase VIII) and D (phases VII and VIII), isotropic thermal displacement factors, and profile coefficients. The instrumental parameters which determine the conversion from time-of-flight to d spacing were determined by refining a pattern of a SRM 640d silicon powder sample from NIST, collected in the respective cycles, and imposing the lattice parameter to 5.431625 Å as recommended by the sample certificate. This procedure ensures that all lattice parameters cited in this paper are calibrated against the Si standard for which the lattice parameters are accurate to 2×10^{-4} Å. The pressure values were obtained from the refined lattice parameters of Pb using its equation of state published in Ref. [19] and an ambient pressure lattice parameter of 4.95216 Å as determined in a separate measurement on the same instrument. An important detail concerns pressure/temperature changes: to minimize potential nonhydrostatic strains all pressure changes were carried out at room temperature, followed by cooling at constant load which results in essentially isochoric temperature variation. Temperatures were measured with an accuracy better than ± 1 K by two thermocouples attached to each anvil at a distance of 10 mm from the sample. The results of the refinements are summarized in Table I for ice VII and Table II for ice VIII at 93 and 196 K.

The $V(P)$ data (Tables I and II) were then fitted to three equation of state relations. With the definitions $X = (V/V_0)^{(1/3)}$, the bulk modulus at ambient pressure $B_0 = -(\partial P/\partial \ln V)_0$, and its pressure derivative $B'_0 = (\partial B_0/\partial P)$, these are:

(1) A third-order Birch equation [25] ("Birch-Murnaghan" EoS, in the following abbreviated as "BM"):

$$P(V) = \tfrac{3}{2}B_0[X^{-7} - X^{-5}]\left[1 - \tfrac{3}{4}(4 - B'_0)(X^{-2} - 1)\right] . \quad (1)$$

TABLE II. Measured lattice parameters of ice VIII and Pb at 93 and 196 K and corresponding pressures.

Run	T (K)	V_{VIII} (Å^3)	a_{Pb} (Å)	P (GPa)
30608	93	143.97(2)	4.841(1)	2.75(2)
30625	93	136.26(3)	4.791(1)	4.83(4)
30636	93	129.49(2)	4.738(1)	7.39(5)
30659	93	121.42(2)	4.669(1)	11.48(7)
30608	196	144.17(2)	4.843(1)	3.00(2)
30625	196	136.37(3)	4.793(1)	5.05(4)
30636	196	129.57(3)	4.740(1)	7.60(5)
30659	196	121.53(3)	4.670(1)	11.63(7)

For $B_0^{\mathrm{t}} = 4$, this relation reduces to the "second-order Birch-Murnaghan" EoS, often simply called "Birch-EoS".

(2) Rydberg-Vinet EoS [26], in the literature mostly called "Vinet" EoS and in the following abbreviated as "RV":

$$P(V) = \frac{3B_0}{X^2}(1 - X)\exp\left[\frac{3}{2}(B_0^{\mathrm{t}} - 1)(1 - X)\right]. \quad (2)$$

(3) Holzapfel's AP1 EoS [27], formerly denoted as H11 [28], and in the following abbreviated as "AP1":

$$P(V) = \frac{3B_0}{X^5}(1 - X)\exp\left[\frac{3}{2}(B_0^{\mathrm{t}} - 3)(1 - X)\right]. \quad (3)$$

In this analysis we deliberately exclude the simple Murnaghan equation [29] due to its well-known shortcomings. This relation implies a volume-independent B^{t} which leads to an unrealistic $V(P)$ at compression ratios V/V_0 smaller than ≈0.9, see Ref. [30] for a detailed discussion on this issue. Since compression ranges in our experiments are as small as 0.7%, the Murnaghan equation is clearly an inappropriate choice.

Fits to the data were carried out with the program DatLab [31], and checks were made using two other commercial softwares. These gave slightly different results, though consistent within the errors, probably due to details of the numerical implementation.

I. ICE VII

Results for ice VII are plotted Fig. 3 in which we include for comparison two other recently published measurements on ice VII. These are neutron powder diffraction data [14] measured between 2 and 6.7 GPa, and x-ray powder data collected in a DAC between 2.7 and 9.8 GPa [15]. We regard these two data sets as the most trustworthy $V(P)$ in the 2–10 GPa range, compared to previous measurements which mostly focused on pressures in the Mbar range [4,5,7,8,11].

Figure 3 reveals a remarkable agreement between our neutron data and those of Fortes *et al.* [14], despite the fact that they were obtained on different instruments, at different neutron sources. The reported EoS by Bezacier *et al.* [15] gives systematically larger unit cell volumes, up to ≈0.7% at ≈5 GPa, equivalent to a difference in pressure of 0.4 GPa.

In an initial analysis, the parameter V_0 was included in the fits which gave (B_0, B_0^{t}, V_0) values of (14.1 ± 1.1 GPa, 5.8 ± 0.3, 42.2 ± 0.3 Å^3) for BM, (13.3 ± 1.0 GPa, 6.3 ± 0.3, 42.3 ± 0.2 Å^3) for RV, and (13.7 ± 1.0, 6.1 ± 0.3, 42.3 ± 1.2 Å^3) for AP1, with all errors corresponding to 68% confidence limit. From this it is immediately evident that the value of V_0 is close to 42.2 Å^3 and that the bulk modulus of ice VII is approximately 13–14 GPa, irrespective of the EoS relation used. Given the remarkable agreement of the V_0 value found by all three EoS forms $V_0 = 42.25$ Å^3 was imposed in the subsequent analysis. This gives final results on B_0, B_0^{t} and V_0 as shown in Table III.

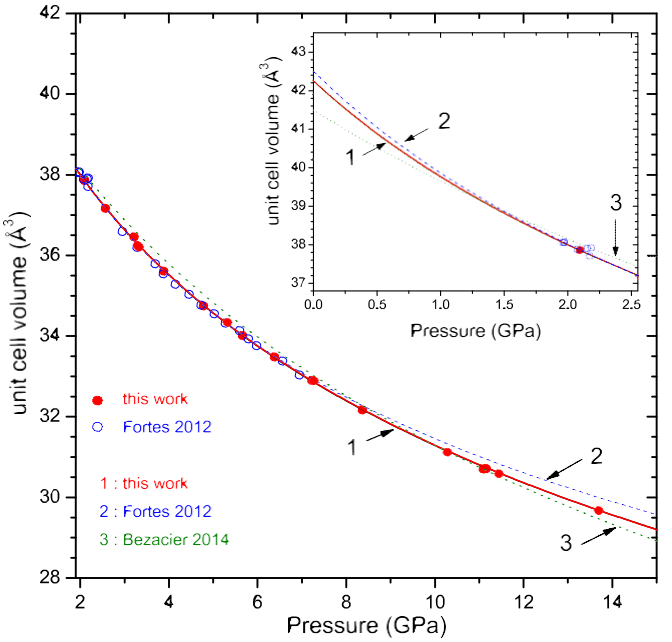

FIG. 3. Pressure dependence of unit cell volume of ice VII. Dots and circles are measured data, lines are fits to our data [Eqs. (1), (2), and (3), not distinguishable over this pressure range] and previously published EoS relations [14,15]. Inset: Enlarged 0–2.5 GPa range with extrapolations of fits to 0 GPa.

In order to gauge how far this EoS is extendable in pressure we show in Fig. 4 $P(V)$ curves extrapolated to 100 GPa (1 Mbar) and compare it with three data sets obtained in diamond anvil cells [4,7,11]. We first recognize the considerable scattering of the data, both within a given data set as well as between different experiments. In the low pressure range up to 10 GPa the data by Wolanin *et al.* [7], which were corrected for nonhydrostatic stresses, agree rather well with our neutron results and the agreement with the extrapolated EoS holds to at least ≈20 GPa. Above ≈25 GPa, the scattering of the data is considerable and no clear conclusion can be

TABLE III. Final results of fits to $V(P)$ data of ice VII (Table I) using three different equations of state. A value $V_0 = 42.25$ Å^3 at 298 K was imposed in the fit as explained in the text.

	B_0 (GPa)	B_0^{t}	V_0 (Å^3)
Third-order Birch	13.8(2)	5.9(1)	42.25
Rydberg-Vinet	13.6(2)	6.2(1)	42.25
Holzapfel AP1	13.7(1)	6.0(1)	42.25

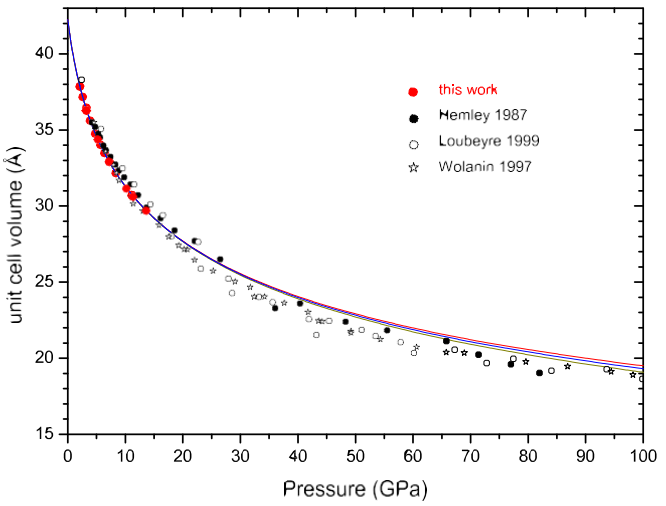

FIG. 4. Pressure dependence of unit cell volume of ice VII with extrapolations to 100 GPa [upper: Eq. (1), middle: Eq. (3), and lower: Eq. (2)], compared to three data sets from x-ray diffraction in diamond anvil cells [4,7,11].

drawn on which result is the most accurate. Above ≈30 GPa the x-ray volumes appear to be on average below our EoS, a fact which hardly can be ascribed to the ice VII-ice X transition [12,13] which occurs between 60 and 70 GPa [8]. What is clear, on the contrary, it that for pressures >85 GPa, the agreement with the x-ray data becomes better and this holds to 160 GPa (not shown in Fig. 4), the highest pressure attained by Wolanin *et al.* [7] and Loubeyre *et al.* [11]. In overall it can be concluded that, despite being established on data in the 0–13.7 GPa range, our EoS extrapolates rather well up to at least ≈30 GPa, possibly even higher, and therefore covers a large part of the stability range of ice VII.

It is clear from these measurements that, whatever the choice of the EoS relation, the zero pressure bulk modulus B_0 of ice VII is approximately 14 GPa or slightly smaller, and its derivative B'_0 between 5.9 and 6.2. This places our B_0 on the lower edge compared to most previous diffraction experiments; consequently, our B'_0 is larger than reported in the majority of these investigations. However, our predicted bulk moduli fit almost perfectly the $B(P)$ dependence obtained from Shimizu's *et al.* Brillouin scattering measurements [6] to at least 7 GPa. We note that these measurements determine bulk moduli (adiabatic, which can be converted to isothermal values) without a fit to EoS relations, i.e., a comparison with results from such model-independent methods is particularly relevant.

II. ICE VIII

Results of the refinements of ice VIII patterns at 93 and 196 K (Table II) are plotted in Fig. 5. This plot includes for comparison the only two published measurements on ice VIII, i.e., x-ray powder diffraction data by Pruzan *et al.* [8] and Yamawaki *et al.* [10]. The former were obtained on cold-compressed samples which might explain the larger deviation from our data compared to the results of Yamawaki *et al.*

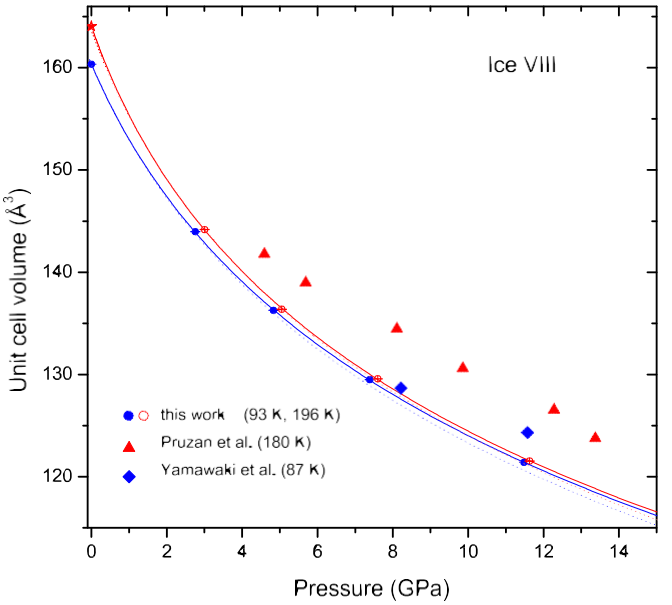

FIG. 5. Pressure dependence of unit cell volume of ice VIII at 93 and 196 K. High pressure data (dots and circles) are from Table II. The two 0 GPa data points correspond to a measured value from recovered samples (93 K) as well an estimated value (196 K) from an interpolation scheme, see Fig. 6 and text. The solid lines are fits to a Rydberg-Vinet EoS [Eq. (2)] and the dotted lines correspond to expected $V(P)$ based on the EoS of ice VII. Published x-ray data at approximately the same temperatures are shown for comparison [8,10].

Similar to the analysis of ice VII, the data were fitted for each temperature to three EoS forms which gave results listed in Table IV. In the 93 K data set we included an ambient pressure value of 160.35 Å^3 determined from neutron diffraction measurements at ISIS on a recovered sample at this temperature [32], see the discussion further below. Since fits to this data set gave V_0 values which deviate by only 0.01 Å^3, V_0 = 160.35 Å^3 was imposed in the final analysis. For the 196 K isotherm, only the high pressure data were included in the fits. These gave fitted V_0 values which are less

TABLE IV. Final results of fits to $V(P)$ data of ice VIII (Table II) using three different equations of state. Values of V_0 = 160.35 Å^3 at 93 K and V_0 = 164.05 Å^3 at 196 K were imposed in the fits as explained in the text.

	B_0 (GPa)	B'_0	V_0 (Å^3)
Third-order Birch			
93 K	18.7(2)	5.7(1)	160.35
196 K	15.6(3)	6.2(2)	164.05
Rydberg-Vinet			
93 K	18.5(2)	6.0(1)	160.35
196 K	15.4(2)	6.4(2)	164.05
Holzapfel AP1			
93 K	18.6(2)	5.9(1)	160.35
196 K	15.6(3)	6.2(2)	164.05

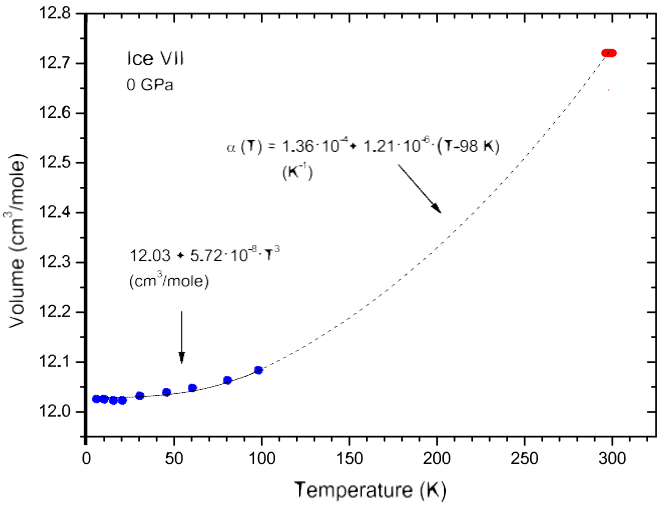

FIG. 6. Thermal expansion of ice VII at ambient pressure. Dots are measured values on recovered samples [16,32], the square is the V_0 value of ice VII at 300 K. The line is an extrapolation as explained in the text.

constrained, but nevertheless differed by only 0.1 Å^3. A value of $V_0 = 164.05$ Å^3 was therefore imposed in the final analysis.

Due to the limited number of pressure points the error bars on V_0, B_0, and B^t_0 are larger than in the case of ice VII, in particular for the 196 K isotherm where no measured V_0 value is available. However, it is beyond uncertainty that the bulk modulus substantially increases with decreasing temperature—as expected—to reach approximately 18.5 GPa at 93 K. The situation is less clear for B^t_0 which appears to have little temperature dependence, if at all.

It was pointed out by Besson *et al.* [33] that an EoS established for ice VII must also hold for ice VIII, at least close to ≈270 K. The reason is that the VII-VIII transition line has a slope $dT/dP = 0$ with a relative volume difference between the two phases smaller than 10^{-3}. Even beyond ≈15 GPa, the experimental evidence of a significant volume difference is weak. This means that, above (in ice VII) and below (in ice VIII) the transition line, the equations of state must be strictly identical. If the thermal expansion of ice VII is known, its EoS can therefore be extended to low temperatures using the Vinet formalism [26]. This allows a direct comparison between ice VII and ice VIII and to gauge to which extent an EoS common to both phases can be established.

For this purpose we use $V(T)$ neutron diffraction data of recovered ice VII collected in the 6–100 K range at ISIS [16,32] and parametrized them by an empirical $\propto T^3$ law as shown Fig. 6. Above 100 K, where recovered ice VII is unstable, we assume a linear behavior of the thermal expansion coefficient $\alpha(\mathrm{T}) = 1.36 \times 10^{-4}\ \mathrm{K}^{-1} + 1.21 \times 10^{-6}\ \mathrm{K}^{-2} \times (T - 98\ \mathrm{K})$. When integrated, the resulting $V(T)$ curve connects to $V_0 = 42.25$ Å^3 (12.72 cm^3/mol) at 298 K as required by our high pressure measurements discussed above. It gives an expansivity of 3.8×10^{-4} K^{-1} at ambient temperature which agrees within ≈50% to values found in ice phases Ih and VI [14] but which is significantly larger than values cited in Refs. [5,9] for ice VII. With this thermal expansion, the temperature dependence of $B_0(T)$ and B^t_0 is then given in the Vinet formalism [26] by

$$B_0(T) = \frac{B_0}{X^2}\,[2 + (\eta - 1)X - \eta X^2]\exp[\eta(1 - X)], \quad (4)$$

$$B^t_0(T) = \frac{4 + (3\eta - 1)X + \eta(\eta - 1)X^2 - \eta^2 X^3}{3[2 + (\eta - 1)X - \eta X^2]}, \quad (5)$$

where $\eta = 3/2(B^t_0 - 1)$, $X = [V(T)/V_0]^{1/3}$, and B_0, B^t_0, and V_0 are the usual ambient condition values (0 GPa, 298 K) as defined above. For $T = 93$ K ($V_0 = 12.07$ cm^3/mol) this analysis predicts for ice VII $B_0 = 18.5$ GPa and $B^t_0 = 5.7$, and for $T = 196$ K ($V_0 = 12.32$ cm^3/mol) $B_0 = 16.5$ GPa and $B^t_0 = 5.9$. The corresponding $V(P)$ curves are shown in Fig. 5 as dotted lines. In the low pressure range up to ≈5 GPa the agreement with the measured data on ice VIII is remarkable, in particular for the 93 K isotherm where the predicted and measured bulk moduli coincide within experimental error, i.e., $B_0 = 18.5$ GPa. Note that this isotherm makes no assumption on the thermal expansion coefficient since it uses only the measured V_0(93 K) value to determine B_0 and B^t_0. Above ≈7 GPa the deviations seem to become significant, at least for the 93 K isotherm. This is obviously related to the fact that at low temperatures the measurements find a larger B^t_0 for ice VIII than expected from an extrapolation of the EoS of ice VII. In other words, the ambient pressure bulk moduli are undistinguishable, but under pressure ice VIII becomes stiffer, at sufficiently low temperatures. The limited number of data points does not allow a firm conclusion but—if confirmed—this potential anomaly in the EoS could well be related to the anomalous stiffening of phonon modes observed in the same P/T range in infrared measurements and first-principles calculations [34]. Its microscopic origin is believed to be in a subtle pressure-induced phonon instability which was reported [34] to have also an effect on the equation of state of ice VIII. The neutron data also observe an anomaly in the c/a ratio (not shown) which might be related to this phenomenon.

III. DISCUSSION AND CONCLUSIONS

The values of B_0 we find for ice phases VII and VIII, i.e., 13–18 GPa, are consistent with the fact that ice Ih has a bulk modulus B_0 of 8.5 GPa [35] and general observations on how bulk moduli scale with density. Apart from very few exceptions which involve solids with electronic transitions, the bulk modulus of a high pressure phase is always larger than of its low pressure phase, see Anderson and Nafe [36] for a systematic study an numerous oxides, halides, and semiconductors. Although hydrogen-bonded systems were not investigated there, it is unquestionable that a similar relation holds for ice phases, i.e., one would expect B_0(Ih) < B_0(VI) < B_0(VII). A B_0 value for ice VII smaller than that of ice Ih [11–13] despite a 56% larger density (12.62 vs 19.64 cm^3/mol for ice Ih) is highly unlikely, if not impossible. Similar arguments might be applied to B^t_0: Strong covalent bonds tend to show values close to 4 or smaller, weaker metallic and van der Waals bonds values between 4 and 7. Again, our B^t_0 = 5.7–6.2 is physically reasonable, given the value for ice Ih which ranges between 5.4 and 6.6, determined from ultrasonic and neutron diffraction measurement, see Ref. [37] and references therein.

A comparison of the elastic properties of the two phases at a given temperature shows no significant difference below ≈7 GPa (Fig. 5). This demonstrates that hydrogen ordering has a very small effect on the bulk modulus, and a similar situation is expected for other ice phases which are related to each other by hydrogen-ordering phenomena, such as ices II and IX. This observation seems to confirm the general belief that the bulk modulus of a solid is determined essentially by density, i.e., that structural details have only a minor effect on B_0 (Ref. [38] and references therein).

The reason for the large scattering among previous diffraction results with a tendency toward overestimating B_0 are multiple: potential presence of strongly nonhydrostatic pressure conditions in DAC experiments [4,7], poor sampling of the low-pressure region [4,7,9,11,12], imposing particular values for B_0 [7,39], for B_0^t [15] or for V_0 [12], or imposing particular EoS relations [14].

Our equation of state of ice VIII differs from the one presented previously by Besson *et al.* [33]. The reason for the significant difference is that Besson's *et al.* EoS [33] was based on Hemley's *et al.* [4] 300 K EoS of ice VII which strongly overestimates the pressure in the 2–25 GPa range, see Fig. 4, hence overestimates significantly the bulk modulus.

Strictly speaking, the equations of state presented here are valid only for deuterated ices VII and VIII. However, the x-ray data of Munro *et al.* [2] demonstrate that there is no detectable difference between the EoS of D_2O and H_2O to at least 30 GPa, and Shimizu's *et al.* Brillouin results to 7.5 GPa come to the same conclusion [6]. We note as well that a potential difference in V_0 between recovered D_2O and H_2O samples is at most 0.04 cm^3/mol for ice VII and 0.02 cm^3/mol for ice VIII [40], i.e., smaller than 0.3%.

In conclusion, we have carried out neutron diffraction experiments to determine the equation of state of ice VII at 298 K between 2 and 13.7 GPa, as well as the EoS of ice VIII to 11.6 GPa and down to 93 K. Fits to these data sets using various EoS relations can reproduce the elastic behavior of ice VII to at least 20 GPa, and possibly even much higher, by comparison with accurate low-pressure neutron data to 6.7 GPa [14] and x-ray data obtained in DACs up to 100 GPa [8,11]. In the 0–7 GPa range, the equations of state of the two phases are indistinguishable, using a Rydberg-Vinet description with the thermal expansion determined from recovered ice VII samples. For higher pressures we find evidence of a small but significant deviation of the two equations of state at low temperatures which we attribute to an anomalous stiffening of phonon modes in ice VIII reported previously [34]. We believe that these equations of state provide the most accurate description of the thermoelastic behavior of the dominant high pressure ice phases currently available.

ACKNOWLEDGMENTS

This work is based on experiments performed at the Japanese neutron spallation source MLF under proposal number 2016I0011 and was supported by JSPS KAKENHI Grants No. 26246039 and No. 15K21712. S.K. is grateful for beamtime obtained at ISIS (Rutherford Appleton Laboratory, Chilton, Didcot, U.K.) in 1999 to collect the low temperature data shown in Fig. 6 and to J. S. Loveday for help during these measurements. We acknowledge helpful discussions with K. Syassen (MPI Stuttgart) who also made the *DatLab* [31] software available to the Paris group.

[1] B. Olinger and P. M. Halleck, J. Chem. Phys. **62**, 94 (1975).
[2] R. G. Munro, S. Block, and F. A. Mauer, and G. Piermarini J. Appl. Phys. **53**, 6174 (1982).
[3] L.-G. Liu, Earth Planet. Sci. Lett. **61**, 359 (1982).
[4] R. J. Hemley, A. P. Jephcoat, H.-K. Mao, C. S. Zha, L. W. Finger, and D. E. Cox, Nature (London) **330**, 737 (1987).
[5] Y. W. Fei, H.-K. Mao, and R. J. Hemley, J. Chem. Phys. **99**, 5369 (1993).
[6] H. Shimizu, T. Nabetani, T. Nishiba, and S. Sasaki, Phys. Rev. B **53**, 6107 (1996).
[7] E. Wolanin, Ph. Pruzan, J. C. Chervin, B. Canny, M. Gauthier, D. Häusermann, and M. Hanfland, Phys. Rev. B. **56**, 5781 (1997).
[8] Ph. Pruzan, J. C. Chervin, E. Wolanin, B. Canny, M. Gauthier, and M. Hanfland, J. Raman Spectroscop. **34**, 591 (2003).
[9] M. R. Frank, Y. Fei, and J. Hu, Geochim. Cosmochim Acta **68**, 2781 (2004).
[10] H. Yamawaki, H. Fujihasa, M. Sakashita, A. Nakayama, and K. Aoki, Physica B **344**, 260 (2004).
[11] P. Loubeyre, R. LeToullec, E. Wolanin, M. Hanfland, and D. Häusermann, Nature (London) **397**, 503 (1999).
[12] E. Sugimura, T. Iitaka, K. Hirose, K. Kawamura, N. Sata, and Y. Ohishi, Phys. Rev. B. **77**, 214103 (2008).
[13] Y. Asahara, K. Hirose, Y. Ohishi, N. Hirao, and M. Murakama, Earth Planet. Sci. Lett. **299**, 474 (2010).
[14] A. D. Fortes, I. G. Wood, M. G. Tucker, and W. G. Marshall, J. Appl. Crystallogr. **45**, 523 (2012).
[15] L. Bezacier, B. Journaux, J.-P. Perrillat, H. Cardon, M. Hanfland, and I. Daniel, J. Chem. Phys. **141**, 104505 (2014).
[16] S. Klotz, J. M. Besson, G. Hamel, R. J. Nelmes, J. S. Loveday, and W. G. Marshall, Nature (London) **398**, 681 (1999).
[17] S. Klotz, J. M. Besson, and G. Hamel, High Press. Res. **26**, 277 (2006).
[18] Y. Wang, D. J. Weidner, and Y. Meng, *Properties of the Earth and Planetary Materials at High Pressure and High Temperature*, Geophysical Monograph Vol. 101 (American Geophysical Union, 1998), p. 365.
[19] Th. Strässle, S. Klotz, K. Kunc, V. Pomjakushin, and J. S. White, Phys. Rev. B. **90**, 014101 (2014).
[20] T. Hattori *et al.*, Nucl. Instrum. Meth. Phys. Res. A **780**, 55 (2015).
[21] S. Klotz, J. M. Besson, G. Hamel, R. J. Nelmes, J. S. Loveday, W. G. Marshall, and R. M. Wilson, Appl. Phys. Lett. **66**, 1735 (1995).
[22] S. Klotz, G. Hamel, and J. Frelat, High Press. Res. **24**, 219 (2004).

[23] K. Komatsu, M. Moriyama, T. Koizumi, K. Nakayama, H. Kagi, J. Abe, and S. Hario, High Press. Res. **33**, 208 (2013).
[24] J. Rodríguez-Carvajal, Physica B **192**, 55 (1993); http://www-llb.cea.fr/fullweb/powder.htm.
[25] F. Birch, J. Appl. Phys. **9**, 279 (1938).
[26] P. Vinet, J. R. Smith, J. Ferrante, and J. H. Rose, Phys. Rev. B **35**, 1945 (1987).
[27] W. B. Holzapfel, High Press. Res. **16**, 81 (1998).
[28] O. Schulte and W. B. Holzapfel, Phys. Rev. B **52**, 12636 (1995).
[29] F. D. Murnaghan, Am. J. Math. **59**, 235 (1937).
[30] K. Syassen, *Isothermal EOS Functions for Solids* (Max-Planck-Institut, Stuttgart, 2012), unpublished.
[31] K. Syassen, *DatLab Computer Code* (Max-Planck-Institut, Stuttgart, 2005).
[32] S. Klotz, ISIS Experimental Report 1999, RB 10412, Rutherford-Appleton Laboratory, Chilton, Didcot, UK.
[33] J. M. Besson, Ph. Pruzan, S. Klotz, G. Hamel, B. Silvi, R. J. Nelmes, J. S. Loveday, R. M. Wilson, and S. Hull, Phys. Rev. B **49**, 12540 (1994).
[34] D. D. Klug, J. S. Tse, Z. Liu, X. Gonze, and R. J. Hemley, Phys. Rev. B **70**, 144113 (2004).
[35] R. Feistel and W. Wagner, J. Phys. Chem. Rev. Data **35**, 1021 (2006).
[36] O. L. Anderson and J. E. Nafe, J. Geophys. Res. **70**, 3951 (1965).
[37] Th. Strässle, S. Klotz, J. S. Loveday, and M. Braden, J. Phys.: Condens. Matter **17**, S3033 (2005).
[38] L. Glasser, Inorg. Chem. **49**, 3424 (2010).
[39] Note that $B_0 = 14.9$ GPa was imposed in the data analysis of Ref. [7]. A three-parameter fit in the 0–13 GPa range gives $B_0 = 27.8$ GPa [7]. The data of this paper are identical to the one of a later work by Pruzan *et al.* [8].
[40] S. Klotz, Th. Strässle, C. G. Salzmann, J. Philippe, and S. F. Parker, Europhys. Lett. **72**, 576 (2004).